Earth, Planets and Space

FULL PAPER

Open Access

CrossMark

Thermo-optical simulation and experiment for the assessment of single, hollow, and large aperture retroreflector for lunar laser ranging

Hiroshi Araki[1*], Shingo Kashima[1], Hirotomo Noda[1], Hiroo Kunimori[2], Kouta Chiba[3], Hitomi Mashiko[3], Hiromasa Kato[3], Toshimichi Otsubo[4], Yoshiaki Matsumoto[5], Seiitsu Tsuruta[6], Kazuyoshi Asari[6], Hideo Hanada[6], Susumu Yasuda[7], Shin Utsunomiya[1] and Hideo Takino[8]

Abstract

A single aperture and hollow retroreflector [corner-cube mirror (CCM)] that in principle has no internal optical path difference is a key instrument for achieving lunar laser ranging one order or more accurate than the current level (~2 cm). We are developing CCM whose aperture is 20 cm with optimized dihedral angles. The 20-cm CCM yields two times peak height for returned laser pulse compared with Apollo 15's retroreflector. Two investigations were conducted to confirm the feasibility of the 20-cm aperture CCM. The first is thermo-optical simulation and evaluation of the 20-cm CCM in the lunar thermal environment. Through this simulation, it has turned out for the first time that 20-cm aperture CCM made of single-crystal Si or "ultra-low expansion glass–ceramics" such as CCZ-EX® (OHARA Inc.) can be used for CCM with no thermal control, if the perfectly fixed point of CCM is limited to one. The second is annealing and shear loading experiments of single-crystal silicon (Si) samples. Through these experiments, high-temperature annealing from 100 to 1000 °C is confirmed to be effective for the enhancement of the adhesive strength between optically contacted surfaces with no optical damage in roughness and accuracy, indicating that this annealing process would enhance the rigidity of CCM fabricated by the optically contacted plates.

Keywords: Lunar laser ranging, Corner-cube mirror, Optical contact, Surface deformation, Fixation, Strehl ratio

Background

LLR and retroreflector on the Moon

Since the first experiment of lunar laser ranging (LLR) in 1969 from McDonald Observatory to Apollo 11 (A11) retroreflector in Mare Tranquilities, LLR has offered unique and invaluable data for nearly half a century. These data have been used as a reference for calculating and establishing numerical or semi-analytical lunar ephemeris. The range accuracy of LLR has been less than 2 cm for the last 20 years owing to the progress of laser transmit/receive system on the ground stations and the

atmospheric signal delay model. Research field related to LLR now covers not only lunar ephemeris but gravitational physics, Earth–Moon dynamics, and precision astrometry (Chapront and Francou 2006). Normal points that are statistically corrected range data are more than 20,000 (http://polac.obspm.fr/llrdatae.html), which include unique and important information for investigating the deep structure of the Moon (Yoder 1981; Williams et al. 2001, 2013).

However, due to the extreme weakness of LLR signals compared with the satellite laser ranging (SLR), only five observatories have succeeded in LLR by now, that is, McDonald, Haleakala, Matera, Côte d'Azur, and Apache Point, and more than 75 % of LLR signals are from the largest retroreflector at the Apollo 15 site (A15) (http://

*Correspondence: araki.hiroshi@nao.ac.jp
[1] National Astronomical Observatory of Japan (NAOJ), 2-21-1 Osawa, Mitaka, Tokyo 181-8588, Japan
Full list of author information is available at the end of the article

Araki *et al. Earth, Planets and Space* (2016) 68:101

Page 2 of 12

ilrs.gsfc.nasa.gov/science/scienceContributions/lunar.html). Therefore, especially for the investigation of the lunar rotational variations, increasing normal point data from retroreflectors as far as possible from the A15 site (Turyshev et al. 2013) is an important goal, in addition to the goal of increasing the range accuracy. Further, it is reported that the reflectivity of lunar reflectors shows degradation by a factor of 10 or more (Murphy et al. 2010), which may affect data accuracy and productivity. To resolve these problems, it is necessary to deploy a new retroreflector whose "reflection performance" (hereafter, we define it as the peak height of received laser pulse over the unit laser output energy with a specified time width) is greater than that of the A15 retroreflector on the lunar southern hemisphere, for example, from the middle to high latitude or lunar peripheral region. In the next section, we describe the 20-cm aperture and hollow-type corner cube as such a new retroreflector model.

Conceptual design of new retroreflector

To yield more reflection performance than A15's retroreflector composed of 300 corner-cube prisms with an aperture of 38 mm, more abundant unit corner-cube prisms must be arrayed. Of course, it is difficult to achieve this, because the size and weight of such an array type retroreflector will surpass the A15 model (Fig. 1). As for the reflection performance, the ray path difference in the A15 retroreflector is already ± 7 cm [± 1 (m) sin 8.2°] due to the array configuration and the optical (lunar orbital) libration, which is the main factor that

Fig. 1 Apollo 15 retroreflector for lunar laser ranging (LLR) (http://www.hq.nasa.gov/office/pao/History/alsj/a15/AS15-85-11468HR.jpg)

limits range accuracy and peak value of returned pulse through the broadening of output laser pulse (Turyshev et al. 2013). "Single-element retroreflector" (SERR) composed of a single corner-cube reflector made of a prism or three mirrors, which has no optical path difference in principle, is considered a solution to overcome these problems. The performance of SERR is determined in principle only by the aperture area. The larger aperture can receive larger signals that allow more precise ranging. There is a detailed report on SERR for LLR (Otsubo et al. 2011), which concludes that SERR whose aperture is 20 cm yields two times reflection performance compared with the A15 retroreflector if a small offset angle [dihedral angle offset (DAO)] being 0.65 ± 0.1 arc second (corresponding to 0.44 ± 0.068 μm offset at the edge of 20-cm SERR) is added to one of three dihedral angles of the SERR. Therefore, we investigate 20-cm aperture SERR hereafter. The aperture diameter of the prism-type SERR is practically limited by the uniformity and thermal property of the prism material as described below; however, the hollow-type SERR is free from such a limitation if the problems relating to deployment and/or environmental problems are solved.

All existing lunar retroreflectors consisting of arrayed corner-cube prisms are more suitable for space use than hollow-type reflectors in terms of stiffness and stability. Recently, a 10-cm aperture corner-cube prism was developed for LLR (Currie et al. 2011); however, it is considered for the 20-cm aperture that inhomogeneity and/or temperature dependency of the refractive index of the prism may cause severe optical degradation in addition to weight and size problems. The optical performance of the 20-cm aperture corner-cube prism made of synthetic quartz is simulated using an evaluation model taking into account the inhomogeneity of prism's refractive index (n) as follows: $\Delta n\,(r, z)/n = 3 \times 10^{-6}\,(z/68)^2\,(r/127.5)^2$, where z (mm) and r (mm) are defined in the cylindrical coordinates (Fig. 2a) and Δn is the variation of "n" of the highest grade synthetic quartz (personal communications with Shin-Etsu Chemical Co., Ltd.). Unfortunately, even on this condition, the 20-cm aperture corner-cube prism shows a severely distorted focal image whose Strehl ratio is 0.02, indicating a poor optical performance (Fig. 2b), where the Strehl ratio is defined as the ratio of focal image peak intensity of the point source between real and perfect optics. Therefore, it is difficult to use the corner-cube prism whose aperture diameter is 20 cm or more as SERR for LLR if we take further the effect of temperature dependence of "n" into account. Thus, we focus on the hollow-type SERR hereafter.

In summary, the following three characteristics required for a new generation LLR retroreflector are derived: (1) SERR, (2) 20 cm aperture with DAO, and
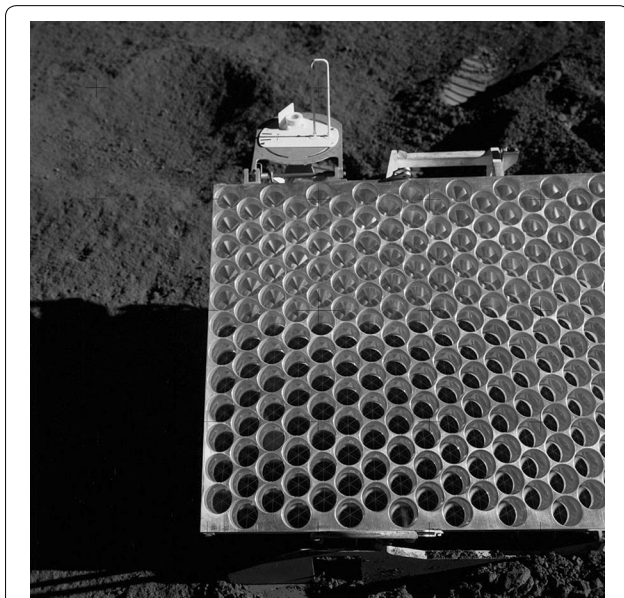
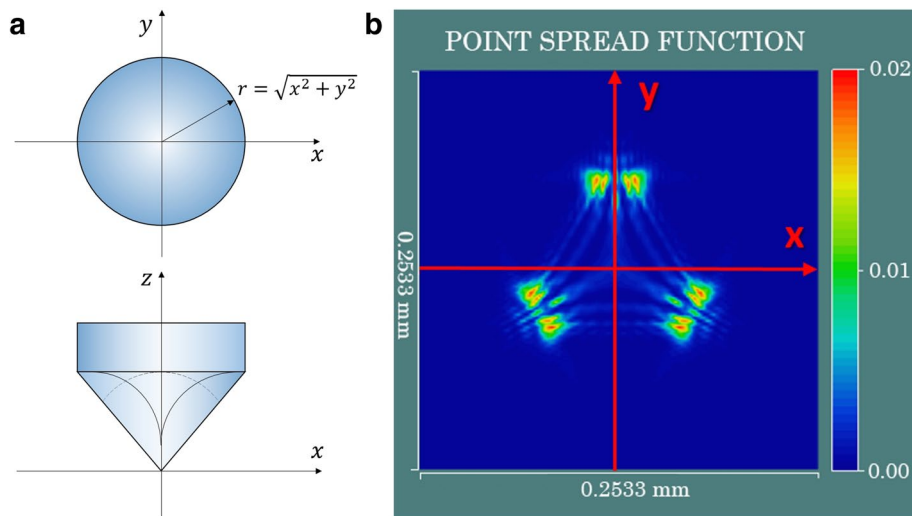Araki *et al. Earth, Planets and Space* (2016) 68:101

Page 3 of 12

Fig. 2 a Coordinate system employed for the formulation of index function of corner-cube prism. See text for explanation. **b** Projected image of the point spread function on the *x–y* plane of corner-cube prism made of synthetic quartz, simulated by the optical design software CodeV 10.6SR1. The image is severely degraded with the Strehl ratio 0.02. See text for more explanation

(3) hollow type. We call the retroreflector being (1) SERR and (3) hollow type as corner-cube mirror (CCM). The deployment of CCM whose aperture is 20 cm on the lunar near side and far from A15 would contribute greatly to the investigation of the lunar precise rotation.

Methods

Two investigations were conducted to confirm the feasibility of the 20-cm aperture CCM as follows, and their results and implications are described from the next section:

[I] Thermo-optical simulation and evaluation of 20-cm aperture CCM in the lunar thermal environment: First, two candidate materials for CCM are sought for higher thermal diffusivity, lower thermal expansion, and higher specific stiffness. Then, surface temperature, deformation, and optical qualities of CCM are simulated using mathematical models of CCM made of the selected materials. Software is Thermal Desktop®, ANSYS®12, and CodeV10.6SR1 for temperature, deformation, and optical simulation, respectively.

[II] Annealing and shear loading experiments of the candidate material, single-crystal silicon (Si): The purpose of these experiments is to confirm whether the annealing may be introduced as post-processing of the optical contact for the CCM fabrication. The optical contact technique is to adhere two surfaces stiffly without using adhesive by contacting and pressing two polished surfaces whose roughness is less than about 1 nm level (Ra). This is suitable for the CCM used in

space without any degassing and contamination from adhesive. Five small Si plates are heated individually to 100, 400, 600, 800, and 1000 °C. Then, the surface accuracy and roughness of these plates are measured and their measurements compared with the pre-annealing measurement data. The optically contacted Si samples were also heated from 100 °C to 1000 °C, and then shear loading was applied to these samples to confirm that the adhesive strength of the optically contacted surface may increase in accordance with temperature as described by Shimbo et al. (1986).

Results and discussion
Material of CCM

CCM on the Moon is exposed to a severe thermal environment with an extremely wide temperature range of about 100 to 400 K (Vasavada et al. 2012). The main concern for this situation is that shadow of CCM cast on itself in the daytime may cause temperature variation and deformation of the CCM surface, leading to the degradation of the optical performance. Thus, it is necessary for the CCM material to have a small coefficient of thermal expansion (C_{TE}) and a large thermal diffusivity (κ) to reduce CCM degradation. $|C_{TE}/\kappa|$ and E/ρ (Young's modulus E/density ρ) of candidate materials for CCM are plotted in Fig. 3. We selected CLEARCERAM™-Z EX (OHARA Inc.; hereafter CCZ-EX®) and single-crystal silicon (Si) as an example of ultra-low expansion glass ceramics and other type material, respectively, but not select HS-SiC even with low $|C_{TE}/\kappa|$ and very high E/ρ because its surface is difficult to polish to the level
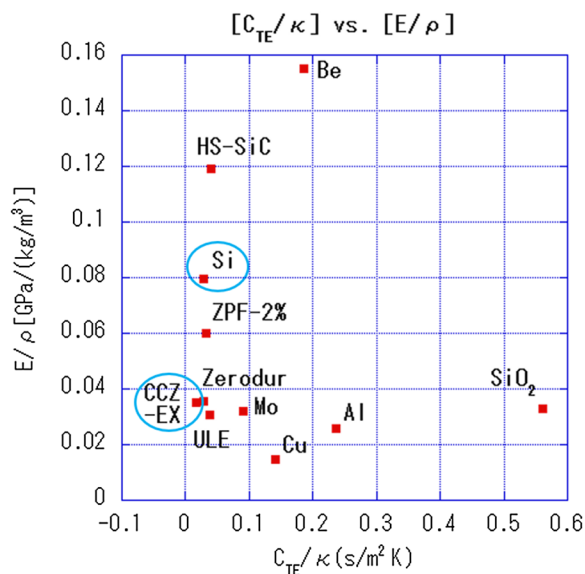
Araki *et al. Earth, Planets and Space* (2016) 68:101

Page 4 of 12

Fig. 3 |C_{TE}/κ| versus (E/ρ) map of several candidate materials for CCM at room temperature, where CCZ-EX® is CLEARCERAM™-Z-EX (OHARA Inc.), ZPF-2 % is zero expansion stiffness ceramics (personnel communication with Nihon Ceratec Co. Ltd.), HS-SiC is high-strength reaction-sintered SiC (Suyama et al. 2003), ULE® is ultra-low expansion glass (Corning Inc.), and Zerodur® is zero expansion glass ceramic' (SHOTT AG). Si and CCZ-EX® are selected for further investigation

where the optical contact technique can be used for the fabrication of CCM. In the next section, simulations are used to examine thermal deformation and optical performance of CCM made of these two materials when they are deployed on the lunar surface in daytime.

Optical performance of CCM on the Moon

We examine the optical performance of CCM made of Si or CCZ-EX® in the lunar thermal environment by the numerical simulation. First, the temperature on the CCM surface is calculated using mathematical model of the whole retroreflector system including CCM ("temperature of CCM surface"). Second, deformation of the CCM surface is calculated based on derived temperature distribution ("deformation of CCM surface"). And third, the optical performance is calculated on the CCM surface deformation ("optical degradation of CCM").

Temperature of CCM surface

Thermal Desktop® software is employed for the calculation of CCM temperature. The mathematical model of the whole reflector system is made of the CCM itself, hemispherical sunshade, supporting frame, tripod, and other parts (Fig. 4). The driver system for turning CCM toward the Earth, which is attached to the back of the tripod, is not taken into account as a heat source for the thermal

calculation, because it is not used during LLR operation. CCM materials are Si or CCZ-EX® as described in chapter "Material of CCM." The shape of the CCM aperture is hexagonal with 141.42 mm length on one side, and thus, the diameter of its inscribed circle is 200 mm. The numerical solid model of CCM for the Thermal Desktop® is gridded to 20 × 20 × 2 nodes to match the scheme of ANSYS®12 software for the subsequent calculation of CCM deformation, where the temperature profile inside the CCM plates (10 mm thickness) is taken into account for accurate calculation. Thermal properties and densities of Si and CCZ-EX® used for the calculation are given in Table 1. Thermal conductivity and specific heat of Si are at 80 °C based on Glassbrenner and Slack (1964), and those of CCZ-EX® are averaged measurements from −150 to +100 °C by AGNE Gijutsu Center Inc. The mirror coating that is the thermal boundary of CCM surface to space is supposed to be silver (Ag; absorption coefficient $\alpha = 0.04$, emissivity $\varepsilon = 0.02$) or aluminum (Al; absorption coefficient $\alpha = 0.25$, emissivity $\varepsilon = 0.04$). Other parts are supposed to be made of carbon fiber-reinforced plastics (CFRP; absorption coefficient $\alpha = 0.8$, emissivity $\varepsilon = 0.89$). Thickness of the hemispherical sunshade, supporting frame, and tripod is 5 mm. Radiative thermal coupling of CCM with lunar surface (albedo 0.07) and space, and conductive thermal coupling are taken into account between "CCM and sunshield," "sunshield and supporting frame," and "tripod and lunar surface" as 0.04 W/K, 0.005 W/K × 2, and 0.045 W/K × 3, respectively.

Surface temperature on the CCM that is set inside Tycho crater (11.2°W, 43.3°S) is calculated, where its optical axis is aligned in the direction of Earth, and self-shadow casting on CCM is taken into account. Heating by solar radiation and lunar reflective radiation is also taken into account assuming that solar radiation constant is 1421 W/m², but radiative heating by the Earth is ignored. Lunar surface temperature profile ranging from about 85 to 365 K at Apollo 17 site (A17; [30° 44′58.3 E, 20° 09′ 50.5 N]) is used for the calculation (Keihm and Langseth 1973). Thus, we should take note that calculated CCM temperature and eventually its deformation shown below are somewhat overestimated because the ground temperature at A17 is higher than at Tycho crater due to the lower latitude of A17 than that of Tycho crater. Results of temperature calculation are summarized in Table 2, and temperature maps on CCM made of Si and CCZ-EX® coated by silver are shown in Fig. 5. Temperature variance becomes much larger for aluminum coating than silver because absorption α of aluminum is larger than silver, indicating that aluminum coating causes larger deformation of CCM surface than silver coating. Therefore, we take silver as the coating material from the next section.
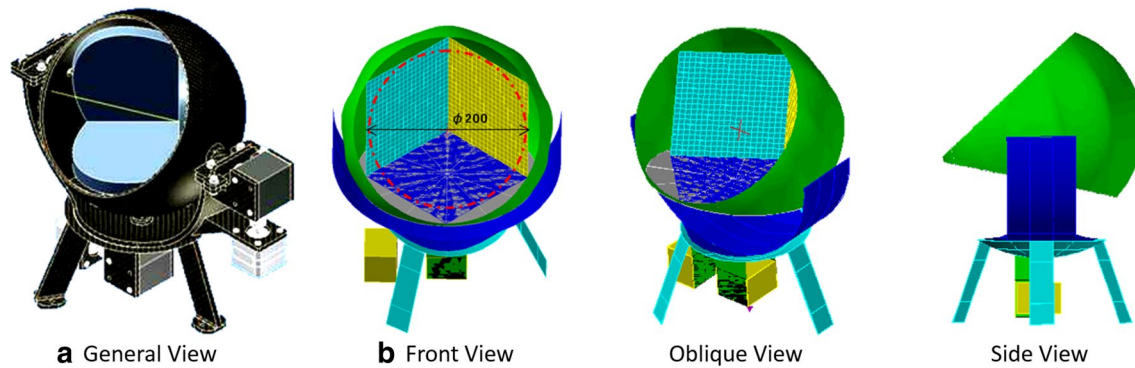
Araki *et al. Earth, Planets and Space* (2016) 68:101

Page 5 of 12

Fig. 4 a General view of the whole reflector model. **b** Mathematical model of the whole reflector system used for the calculation of temperature on CCM surface by Thermal Desktop® software. See text for more explanation

Table 1 Thermal conductivity, specific heat, and density used for the temperature calculation of CCM made of Si and CCZ-EX®

Material	Thermal conductivity (W/m/K)	Specific heat (J/kg/K)	Density (kg/m^3)
Si	125.34	760	2329
CCZ-EX®	1.10	693	2550

Deformation of CCM surface

Deformation of the CCM under the temperature distribution obtained in the previous section is calculated by ANSYS® 12 with the $20 \times 20 \times 2$ mesh numerical model used for the temperature calculation assuming that the surface is perfectly flat when the CCM temperature is 25 °C. Thermal expansion data (C_{TE}) of Si and CCZ-EX® necessary for the calculation are shown in Fig. 6a, b, respectively.

Deformation of CCM surface under the temperature distribution obtained in the previous section is calculated by ANSYS® 12 with 20×20 mesh and with the assumption that the surface is perfectly flat when CCM temperature is 25 °C. Thermal expansion data (C_{TE}) of

Table 2 Results of maximum/minimum surface temperature and their differences on CCM made of Si or CCZ-EX® coated by silver (Ag) or aluminum (Al)

Material	Coating	Maximum temperature (°C, at noon)	Minimum temperature (°C, at noon)	Difference (°C, at noon)
Si	Ag	83.8	83.3	0.5
Si	Al	122.2	120.4	1.8
CCZ-EX®	Ag	100.8	78.4	22.4
CCZ-EX®	Al	197.9	104.8	93.1

CCM surface coated by aluminum shows much larger temperature difference than the surface by silver coating due to large absorption a

single-crystal Si and CCZ-EX® necessary for the calculation are shown in Fig. 8a, b, respectively.

It is anticipated that calculation results may be highly dependent on the way CCM is mounted on the structure (Fig. 4b). Hereafter, we suppose six fixing methods of CCM, that is, [000], [011], [012], [0000], [0112], and [0122], where the former three stand for "three-point fixing" and latter three "four-point fixing," respectively (Fig. 7). The calculation is performed for two materials (Si and CCZ-EX®) and six fixing methods above, that is, for 12 cases in total, where fixed points are the backside of CCM. Density, Young's modulus, and Poisson's ratio of the two materials are given in Table 3, where anisotropy of the elastic properties of Si is taken into account (Wortman and Evans 1965).

Four deformation maps calculated by ANSYS® 12 are shown in Fig. 8 for the case of Si_[000], CCZ-EX®_[000], Si_[011], and CCZ-EX®_[011], where, for example, Si_[000] means that CCM material is Si and the fixing method is [000]. Normal component of surface deformation for the case of Si_[000] is 40 μm at most being more than two orders of magnitude larger value than 78 nm for Si_[011]. Similarly, for the case of CCZ-EX®_[000], the deformation is 1 μm at most being four times larger than 250 nm for CCZ-EX®_[011].

Maximum normal components of surface deformation for all 12 cases are summarized in Table 4. It is clearly shown that perfect multi-point fixation such as [000] or [0000] causes huge surface deformation.

Optical degradation of CCM surface

The optical performance of CCM is evaluated by the calculation of the point spread functions (PSF) and Strehl ratio by CodeV10.6SR1 software. Strehl ratio is considered here to be the ratio of intensity peak of focal image by deformed CCM over the intensity peak value of perfect image by the deformation free CCM. PSF maps are
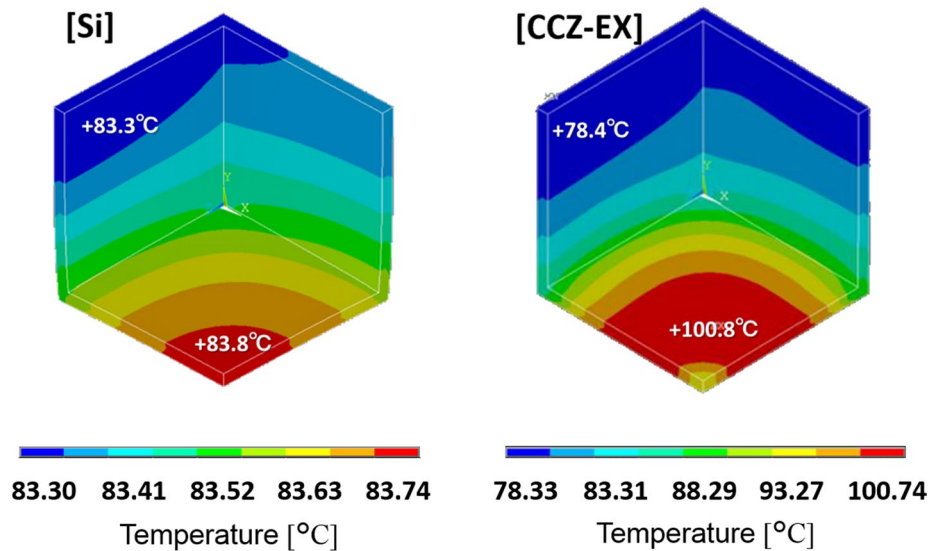
Araki *et al. Earth, Planets and Space* (2016) 68:101

Page 6 of 12

Fig. 5 Temperature distribution on the surface of CCM made of Si or CCZ-EX® with silver coating. Temperature variation is 0.5 degrees for CCM made of Si, whereas it is 22.4° for that made of CCZ-EX®
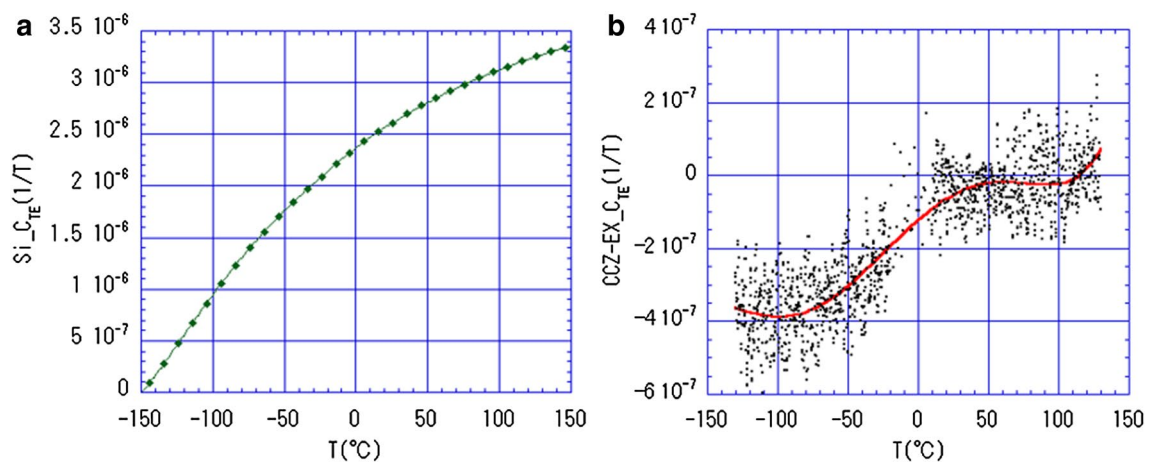

Fig. 6 a Thermal expansion of Si as a function of temperature from White and Minges (1997). **b** Thermal expansion of CCZ-EX® as a function of temperature from our measurement data. *Red line* in **b** is fitted to measured data in the least-squared manner

shown in Fig. 9 for the same cases as Fig. 8, revealing that CCM made of both candidate material (Si or CCZ-EX®) fixed perfectly to the structure on multi-points cannot be used at all for LLR because the optical performance is severely degraded due to the huge deformation of CCM surface. However, when only one point is fixed perfectly and other fixed points have one or two degrees of freedom along the CCM surface, the optical degradation is very small, indicating no problem for LLR use. Strehl ratios are summarized in Table 5, indicating again that perfect fixing on multi-points leads to severe optical degradation of CCM. For the cases other than perfect

multi-point fixation, Strehl ratio is confirmed to be more than about 90 %, and thus there is no optical problem for LLR use.

Optical performance of CCM expected on the Moon

CCM made of Si or CCZ-EX®, deployed inside Tycho crater in the daytime, is heated up to 83.3–83.8 °C or 78.3–100.7 °C, respectively (Fig. 5). The temperature difference within a CCM made of CCZ-EX® is 22.4 °C being much larger than that of CCM made of Si (0.5 °C). However, the deformations of CCM made of Si and CCZ-EX® are comparable, unless the multi-point fixation is
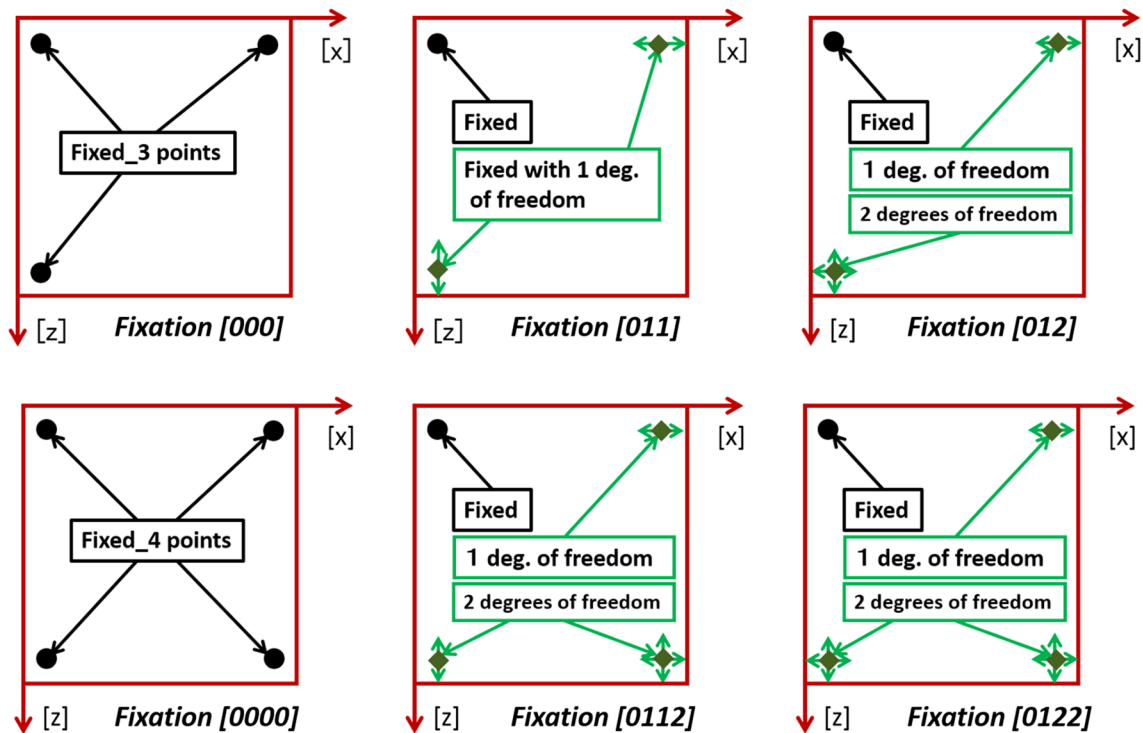
Araki *et al. Earth, Planets and Space* (2016) 68:101

Page 7 of 12

Fig. 7 Six fixation methods of CCM to the holder. The *red square* of *each figure* represents the *backside* of CCM base. CCM deformation is calculated for all these fixation methods and two materials (Si and CCZ-EX®), thus 12 cases in total. The names for fixation are attached under *each figure*. For example, [000] means that three points are fixed perfectly and [012] means that degree of freedom of motion is zero (perfectly fixed), one (motion along one direction other than [z] is allowed), and two (motion within the CCM surface is allowed)

Table 3 Density, Young's modulus, and Poisson's ratio of Si and CCZ-EX® used for the calculation of CCM deformation. Originated from Wortman and Evans (1965)

Material	Density (kg/m³)	Young's modulus (GPa)	Poisson's ratio
Si	2329	185 (111)	0.28 (100)
		170 (110)	0.26 (111)
		130 (100)	
CCZ-EX®	2550	91	0.26

Data for Si are cited from the Web resource (http://www.ioffe.ru/SVA/NSM/Semicond/Si/mechanic.html#Basic)

employed. Actually, for the fixation other than [000] or [0000], maximum normal deformation is 78 or 91 nm for CCM made of Si and 106 or 251 nm for CCM made of CCZ-EX®, respectively (Table 4). This is because $|C_{TE}|$ of Si is much larger than that of CCZ-EX® contrary to the temperature difference between these two materials. Strehl ratios also show good values from 89.7 to 99.3 % for the cases other than [000] or [0000]. Thus, CCM made of these two materials suffers no optical damage unless perfect multi-point fixation ([000] or [0000]) is employed (Table 5). Therefore, if the perfectly fixed point of CCM is

limited to one, CCM made of Si or CCZ-EX® can be used safely for LLR with no thermal control.

As for the perfect multi-point fixation ([000] or [0000]), normal deformation reaches 40–46 μm for CCM made of Si or 0.93–0.99 μm for that made of CCZ-EX®, respectively, where large thermal deformation occurs due to multi-point fixation of the CCM even when slight temperature difference to the reference (25 °C) is applied, which leads to poor Strehl ratios from 4.4 to 7.3 %. Therefore, it is difficult to use CCM being fixed on multi-points for LLR.

However, CCM made of CCZ-EX® shows smaller normal deformation than Si even for the multi-point fixation due to the very small $|C_{TE}|$. For example, the normal deformation of CCM made by CCZ-EX® for [000] fixation is 0.99 μm, which is only about four times larger than the case for [011] fixation (normal deformation is 0.25 μm and the Strehl ratio is 91 %) (Tables 4, 5). Therefore, it may be possible to employ the multi-point fixation method for CCM support if we can use material whose $|C_{TE}|$ is less than 1/4 of CCZ-EX® and thermal diffusivity is the same as CCZ-EX® in future.

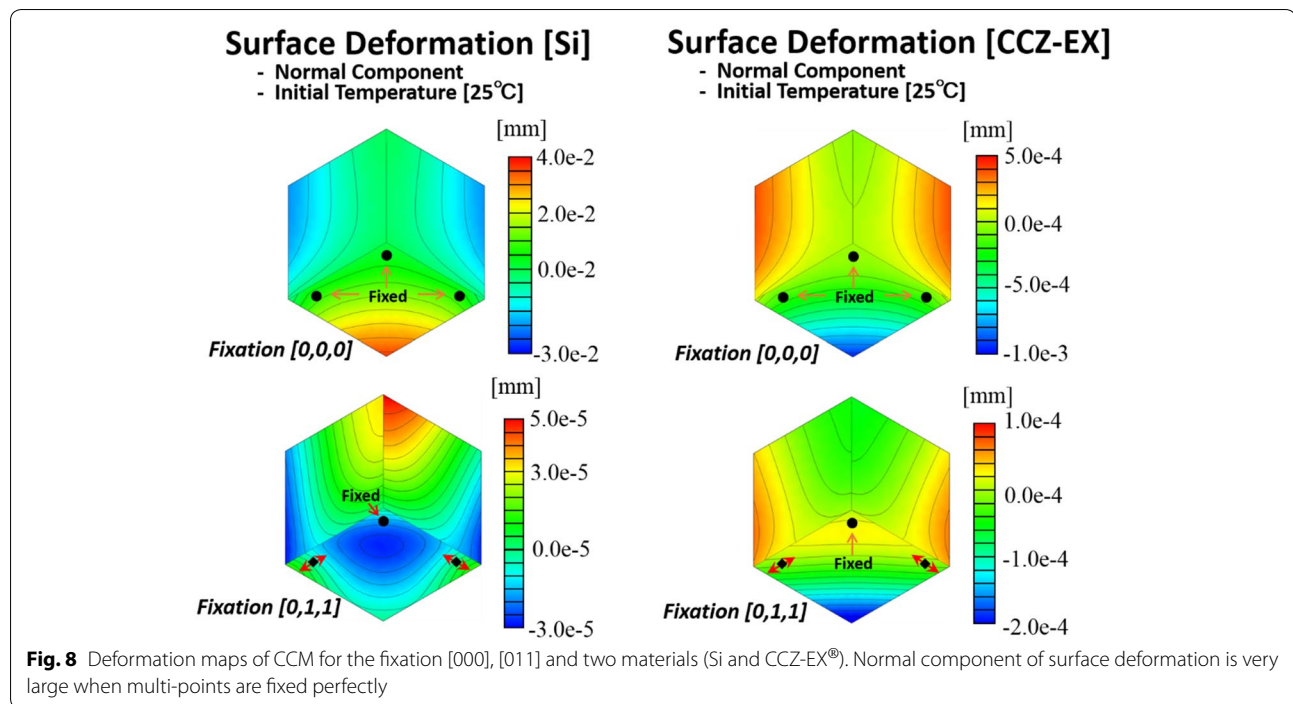In summary, two conclusions are derived on the performance of CCM as follows:

Araki *et al. Earth, Planets and Space* (2016) 68:101

Page 8 of 12

Fig. 8 Deformation maps of CCM for the fixation [000], [011] and two materials (Si and CCZ-EX®). Normal component of surface deformation is very large when multi-points are fixed perfectly

Table 4 Maximum normal deformation of CCM surface for two materials (Si and CCZ-EX®) and six fixation methods (Fig. 7)

Material	Fix_3 [000]	[011]	[012]	Fix_4 [0000]	[0112]	[0122]
Si (μm)	40.17	0.0780	0.0905	46.22	0.7910	0.0909
CCZ-EX® (μm)	0.9900	0.2514	0.1477	0.9295	0.1060	0.1418

Fix_3 and 4 stand for "three-point fixing" and "four-point fixing," respectively
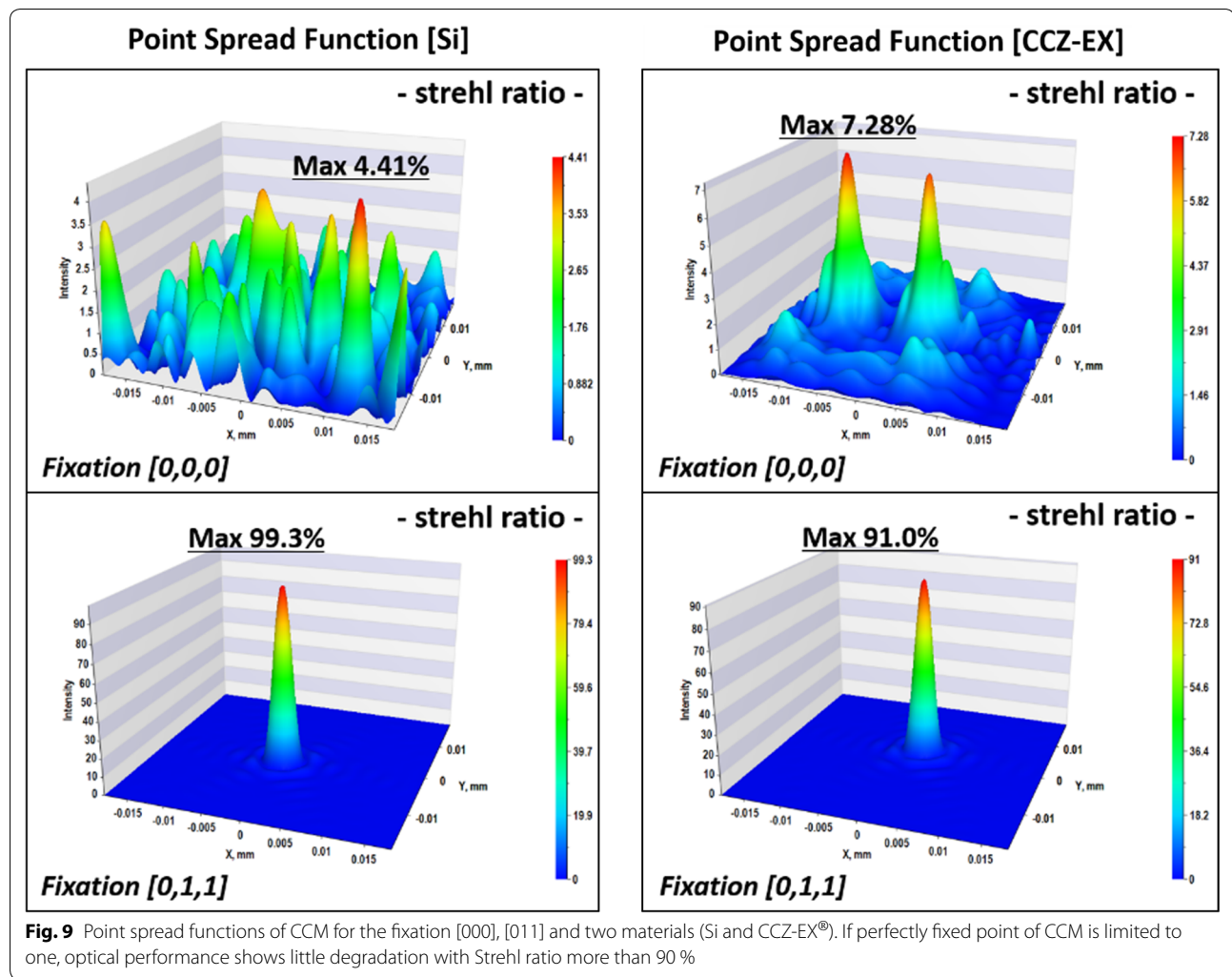
1. Thermal deformation and optical performance of CCM whose aperture is 20 cm are strongly dependent on the fixation method. CCM made of Si and CCZ-EX® can be used for LLR retroreflector with no thermal control on the Moon if the perfectly fixed point of CCM is limited to one.

2. However, it may be possible to introduce the multi-point fixation method for CCM support if in future we can use CCM material whose $|C_{TE}|$ and κ are less than 1/4 of CCZ-EX® and the same as CCZ-EX®, respectively.

Annealing and shear loading experiment of Si test pieces

We investigated whether the optical contact technique with a high-temperature annealing process can be applied to CCM fabrication by conducting experiments with Si test pieces, aiming to solve two problems: (I) how much CCM surface degrades optically by high-temperature annealing and (II) how much improvement of stiffness between optically contacted interface is expected by the annealing process (Noda et al. 2015).

Experiments I and II are conducted corresponding to the above problems (I) and (II), respectively: [Experiment I] Mirror-polished Si plates (<1 nm in RMS surface roughness; 20 mm × 21 mm × 5 mm) were prepared. Before the annealing test, the surface accuracy and roughness were measured using a laser interferometer (ZYGO, GPI XP) and an atomic force microscope (AFM). The same measurements were conducted after the annealing process for comparison. One thing should be noted that the area measured with AFM is 1 micron by 1 micron for each sample, while the position accuracy of AFM is only about 1 mm. Therefore, it is not the case that the same region was measured before and after the annealing. [Experiment II] Five sets of test pieces made of optically contacted three Si plates with the same dimension were prepared (Fig. 10) for the shear loading test so that the center piece could be pushed using a pressurizer (Autograph AG-1, SHIMADZU Corp.) to generate shear stress on both of the optically contacted interfaces.

Five small plates for [Experiment I] and five test pieces for [Experiment II] had been pre-heated to 100 °C during

Araki *et al. Earth, Planets and Space* (2016) 68:101

Page 9 of 12

Fig. 9 Point spread functions of CCM for the fixation [000], [011] and two materials (Si and CCZ-EX®). If perfectly fixed point of CCM is limited to one, optical performance shows little degradation with Strehl ratio more than 90 %

Table 5 Strehl ratios of CCM surface for two materials (CCZ-EX® or Si) and six fixation methods (Fig. 7)

Material	Fix_3 [000]	[011]	[012]	Fix_4 [0000]	[0112]	[0122]
Si	0.044	0.993	0.908	0.061	0.992	0.947
CCZ-EX®	0.073	0.910	0.948	0.066	0.977	0.897

Fix_3 and 4 stand for "three-point fixing" and "four-point fixing," respectively

the optical contact process. They are heated again and annealed for two hours up to 100, 400, 600, 800, and 1000 °C, in the electric furnace, respectively, and then naturally cooled down to the room temperature within half a day or a day. The shear loading test in [Experiment II] was carried out in a box, one side of which is made of transparent acrylic for observation and to prevent test pieces from scattering fragments when ruptured.

Results of [Experiment I] and [Experiment II] are given in Tables 6 and 7, respectively. From [Experiment I], the degradation of surface accuracy is found to be less than $0.003 \lambda_{HeNe}$ (RMS; $\lambda_{HeNe} = 633$ nm) that is small enough to be ignored. The degradation of surface roughness is also slight enough to be ignored being less than 0.1 nm (Ra) that is equivalent to the optical scattering loss less than 6×10^{-5} TIS (total integrated scattering), where TIS $= (4\pi\sigma/\lambda_{532})^2$ in which σ is surface roughness and λ_{532} is wavelength (532 nm). These results suggest that the surface accuracy and roughness of a mirror made of Si show no degradation even in high-temperature
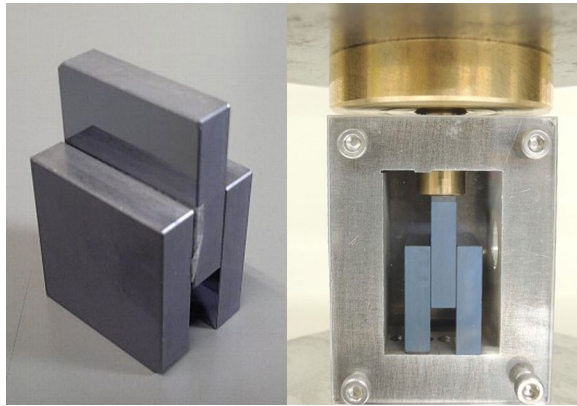
Araki *et al. Earth, Planets and Space* (2016) 68:101

Page 10 of 12

Fig. 10 Test piece for the assessment of optical contact bonding force (*left*). The dimension of each component plate is 20 mm × 21 mm × 5 mm, and three plates are optically in contact with each other. The *middle plate* is *vertically* shifted so that forces can be applied to this plate to generate shear stress on both of the optically contacted interfaces (*right*)

environments up to 1000 °C. [Experiment II] shows that the rupture strength of a test piece generally increases with the maximum temperature exposed during the annealing process and that the adhesive strength of the test piece annealed at 1000 °C is several times larger than that annealed at 100 °C, where "rupture strength" of the piece at 1000 °C is not at ruptured timing but the maximum value during the pushing operation because the test piece was not ruptured during the test (Table 7).

In summary, an additional annealing process up to 1000 °C on the optically contacted CCM element plates is confirmed to enhance the adhesive strength several times without any damage of the optical performance. This annealing process prior to the coating would be a great contribution for the fabrication of CCM.

Table 6 Results of [Experiment I]

Temperature (°C)	Surface accuracy ZYGO interferometer [RMS wave (633 nm)]		Surface roughness AFM [Ra (nm)]	
	Before	**After**	**Before**	**After**
100	0.007	0.007	0.096	0.104
400	0.006	0.006	0.099	0.111
600	0.006	0.006	0.105	0.127
800	0.004	0.007	0.164	0.233
1000	0.010	0.009	0.322	0.225

Surface accuracy and roughness measurements of Si plates. RMS stands for root mean square, and Ra stands for the arithmetic average of absolute topographic height

Table 7 Results of [Experiment II]

Temperature [°C]	Rupture strength (MPa)
100	1.988
400	3.394
600	2.654
800	5.836
1000	>10.04

The rupture strength of test pieces for each annealing temperature from 100 to 1000 °C. Rupture strength at 1000 °C is lower limit because the sample was not ruptured during the test

Conclusion and future prospects

A 20-cm CCM whose reflection performance is twice that of the Apollo 15 reflector on the Moon will bring a breakthrough to LLR and lunar and planetary geodesy through significant improvements in range accuracy, data productivity, and the expansion of the ground station network. In this paper, we have confirmed for the first time that a 20-cm hollow-type SERR (20-cm CCM) can be used for LLR retroreflector in the lunar thermal environment. In addition, we found that the optical contact with high-temperature annealing is effective to enhance the rigidity of CCM.

We have investigated a 20-cm aperture CCM by the thermo-optical simulation. First, a 20-cm SERR made of a corner-cube prism is confirmed to be difficult to use as a lunar retroreflector due to the limit of the material uniformity and/or thermal variation of the refractive index. Then, two important conclusions are derived from our simulation: The first is that a 20-cm aperture CCM made of "single-crystal silicon (Si)" or "ultra-low expansion glass–ceramics" such as CCZ-EX® (OHARA Inc.) can be used as a lunar retroreflector with no thermal control if the perfectly fixed point of CCM is limited to one; the second is that it may be possible to introduce the multi-point fixation method for CCM support if in future we can use CCM material whose $|C_{TE}|$ and κ are less than 1/4 of CCZ-EX® and the same as CCZ-EX®, respectively.

Next, we have conducted annealing experiments from 100 to 1000 °C and shear loading experiments of Si samples and confirmed the efficiency of high-temperature annealing for the enhancement of the adhesive strength between optically contacted surfaces with no optical damage in roughness and accuracy. This annealing process would enhance the rigidity of CCM made of the optically contacted plates.

The remaining important issues on the CCM design are as follows: (1) to search for a tougher coating material than silver with similar thermal properties and reflectivity, (2) to investigate the radioactive affection on the reflectivity and/or deformation of the surface of the

Araki *et al. Earth, Planets and Space* (2016) 68:101

Page 11 of 12

CCM, (3) to assess the electric charging and dust accumulation of CCM surface and its effect on the reflectivity, (4) to investigate fabricating and figuring of CCM with DAO by three plates by using optical contact technique, and finally (5) to establish the process of how to fabricate the whole retroreflector system including secure holding mechanism for CCM. As for (1) or (2), the dielectric coating, whose reflectivity can be adjusted to nearly perfect for a specified wavelength, should be tested for long-term operation because the coating is generally vulnerable to the ultraviolet or radiative environment in space. SiO or SiO_2 (SiOx) coating over the silver one is expected to have more resistivity against the space radiative environment and also has a function to protect the silver coating from the corrosion on the ground, but the long-term resistivity is future issue to be confirmed. (3) is an important issue for the quantitative analysis of return signals of LLR. As for (4) and (5), 20-cm aperture CCM must have DAO being 0.65 ± 0.1 arc second, which requires figuring precision better than several tens of nanometer level. To find and establish how to add DAO on the CCM, we are now investigating the performance and applicability of ion beam figuring (IBF) to our purpose (Allen and Romig 1990; Schindler et al. 2001).

Abbreviations

AFM: atomic force microscope; CCM: corner-cube mirror; CCZ-EX®: CLEARCERAM™-Z EX; CFRP: carbon fiber-reinforced plastics; C_{TE}: thermal expansion coefficient; DAO: dihedral angle offset; HS-SiC: high-strength reaction-sintered SiC; IBF: ion beam figuring; ILRS: International Laser Ranging Service; LLR: lunar laser ranging; SERR: single-element retroreflector; TIS: total integrated scattering; ULE: ultra-low expansion glass; ZPF: zero expansion stiffness ceramics.

Authors' contributions

HA selected candidate materials for CCM, performed optical evaluation of the CCM mathematical model and other optical analyses with SK, conducted the annealing and shear loading experiment of Si test pieces, analyzed data obtained by the experiments, and prepared the manuscript. SK performed optical evaluation of the CCM mathematical model and other optical analyses, conducted the annealing and shear loading experiment of Si test pieces, and contributed a design of CCM configuration. YM calculated surface temperature of CCM model. KC, MH, and HK calculated surface deformation of CCM model. SU and HA measured the coefficient of thermal expansion of CCZ-EX®. SU, SY, ST, and KA contributed the annealing and shear loading experiment of Si test pieces. HN, HH, and HT joined and contributed to the discussion. All authors read and approved the final manuscript.

Author details

[1] National Astronomical Observatory of Japan (NAOJ), 2-21-1 Osawa, Mitaka, Tokyo 181-8588, Japan. [2] National Institute of Information and Communications Technology (NICT), 4-2-1 Nukui-Kitamachi, Koganei, Tokyo 184-8795, Japan. [3] Faculty of Engineering, Iwate University, 3-18-8 Ueda, Morioka, Iwate 020-8550, Japan. [4] Graduate School of Social Sciences, Hitotsubashi University, 2-1 Naka, Kunitachi, Tokyo 186-8601, Japan. [5] PLANET Inc., Light Bldg. 7F, 2-12-3 Ginza, Chuo-ku, Tokyo 104-0061, Japan. [6] National Astronomical Observatory of Japan (NAOJ), 2-12 Hoshigaoka-cho, Ohshu, Iwate 023-0861, Japan. [7] Japan Aerospace Exploration Agency (JAXA), 2-1-1 Sengen, Tsukuba, Ibaraki 305-8505, Japan. [8] Faculty of Engineering, Chiba Institute of Technology, 2-17-1 Tsudanuma, Narashino, Chiba 275-0016, Japan.

References

Allen LN, Romig HW (1990) Demonstration of an ion-figuring process. In: Advanced optical manufacturing and testing, 22, SPIE 1333:22–33. doi:10.1117/12.22786

Chapront J, Francou G (2006) Lunar laser ranging: measurements, analysis, and contribution to the reference Systems. IERS Tech Note 34:97–116

Currie DG, Dell'Agnello S, Delle Monache GO (2011) A lunar laser ranging retroreflector for the 21st Century. Acta Astronaut 68(7–8):667–680. doi:10.1016/j.actaastro.2010.09.001

Glassbrenner CJ, Slack GA (1964) Thermal conductivity of silicon and germanium from 3 K to the melting point. Phys Rev 134(4):1058–1069. doi:10.1103/PhysRev.134.A1058

Keihm SJ, Langseth MG Jr (1973) Surface brightness temperatures at the Apollo 17 heat flow site: thermal conductivity of the upper 15 cm of regolith. Geochim Cosmochim Acta Suppl 4(3):2503–2513

Murphy TW Jr, Adelberger EG, Battat JBR, Hoyle CD, McMillan RJ, Michelsen EL, Samad R, Stubbs CW, Swanson HE (2010) Long-term degradation of optical devices on the moon. Icarus 208:31–35. doi:10.1016/j.icarus.2010.02.015

Noda H, Araki H, Kashima S, Utsunomiya S, Tsuruta S, Asari K, Yasuda S (2015) Thermal tolerance test for the development of a hollow retroreflector for future lunar laser ranging. Paper presented at the 46th Lunar and Planetary Science Conference, The Woodlands Texas, 16-20 March 2015

Otsubo T, Kunimori H, Noda H, Hanada H, Araki H, Katayama M (2011) Asymmetric dihedral angle offsets for large-size lunar laser ranging retroreflectors. Earth Planets Space 63: e13-e16. doi:10.5047/eps.2011.11.001

Schindler A, Haensel T, Flamm Di, Frank W, Boehm G, Frost F, Fechner R, Bigl F, and Rauschenbach B (2001) Ion beam and plasma jet etching for optical component fabrication. In: Lithographic and Micromachining Techniques for Optical Component Fabrication, 217, SPIE 4440:217-227. doi:10.1117/12.448043

Shimbo M, Furukawa K, Fukuda K, Tanzawa K (1986) Silicon-to-silicon direct bonding method. J Appl Phys 60:2987–2989. doi:10.1063/1.337750

Si—Silicon; Mechanical properties, elastic constants, lattice vibrations. http://www.ioffe.ru/SVA/NSM/Semicond/Si/mechanic.html#Basic. Accessed on 3 May 2016

Suyama S, Kameda T, Itoh Y (2003) Development of high-strength reaction-sintered silicon carbide. Diam Relat Mater 12(3–7):1201–1204. doi:10.1016/S0925-9635(03)00066-9

Turyshev SG, Williams JG, Folkner WM, Gutt GM, Baran RT, Hein RC, Somawardhana RP, Lipa JA, Wang S (2013) Corner-cube retro-reflector instrument for advanced lunar laser ranging. Exp Astron 36(1):105–135. doi:10.1007/s10686-012-9324-z

Vasavada AR, Bandfield JL, Greenhagen BT, Hayne PO, Siegler MA, Williams JP, Paige DA (2012) Lunar equatorial surface temperatures and regolith properties from the Diviner lunar radiometer experiment. J Geophys Res 117:E00H18. doi:10.1029/2011JE003987

Araki *et al. Earth, Planets and Space* (2016) 68:101

Page 12 of 12

White GK, Minges ML (1997) Thermophysical properties of some key solids: an update. Int J Thermophys 18(5):1269–1327. doi:10.1007/BF02575261

Williams JG, Boggs DH, Yoder CF, Ratcliff JT, Dickey JO (2001) Lunar rotational dissipation in solid body and molten core. J Geophys Res 106:27933–27968. doi:10.1029/2000JE001396

Williams JG, Boggs DH, Folkner WM (2013) DE430 lunar orbit, physical librations and surface coordinates. In: NAIF planetary data system navigation node, NASA. http://naif.jpl.nasa.gov/pub/naif/generic_kernels/spk/planets/de430_moon_coord.pdf. Accessed on 3rd May, 2016

Wortman JJ, Evans RA (1965) Young's modulus, Shear modulus, and Poisson's ratio in silicon and germanium. J Appl Phys 36:153–156. doi:10.1063/1.1713863

Yoder CF (1981) The free libration of a dissipative Moon. Phil Trans R Soc Lond A 303:327–338